

Title	Emergence of a thread-like pattern with charged phospholipids on an oil / water interface.
Author(s)	Ito, Hiroaki; Yanagisawa, Miho; Ichikawa, Masatoshi; Yoshikawa, Kenichi
Citation	The Journal of chemical physics (2012), 136(20)
Issue Date	2012-05
URL	http://hdl.handle.net/2433/158288
Right	© 2012 American Institute of Physics
Type	Journal Article
Textversion	publisher

Emergence of a thread-like pattern with charged phospholipids on an oil/water interface

Hiroaki Ito, Miho Yanagisawa, Masatoshi Ichikawa, and Kenichi Yoshikawa

Citation: *J. Chem. Phys.* **136**, 204903 (2012); doi: 10.1063/1.4722079

View online: <http://dx.doi.org/10.1063/1.4722079>

View Table of Contents: <http://jcp.aip.org/resource/1/JCPSA6/v136/i20>

Published by the [American Institute of Physics](#).

Additional information on *J. Chem. Phys.*

Journal Homepage: <http://jcp.aip.org/>

Journal Information: http://jcp.aip.org/about/about_the_journal

Top downloads: http://jcp.aip.org/features/most_downloaded

Information for Authors: <http://jcp.aip.org/authors>

ADVERTISEMENT



AIP Advances

Special Topic Section:
PHYSICS OF CANCER

Why cancer? Why physics? [View Articles Now](#)

Emergence of a thread-like pattern with charged phospholipids on an oil/water interface

Hiroaki Ito,¹ Miho Yanagisawa,² Masatoshi Ichikawa,^{1,a)} and Kenichi Yoshikawa¹

¹*Department of Physics, Graduate School of Science, Kyoto University, 606-8501 Kyoto, Japan*

²*Department of Physics, Graduate School of Sciences, Kyushu University, 812-8581 Fukuoka, Japan*

(Received 24 February 2012; accepted 9 May 2012; published online 24 May 2012)

The spontaneous formation of a thread-like pattern with negatively charged lipids on an oil/water interface is reported. An analysis of the time-dependent change at the interface observed by fluorescence microscopy revealed that the thread-like pattern is generated through a two-step mechanism. First, inverted lipid micelles in the bulk-oil phase gradually diffuse onto the oil/water interface. Next, the micelles are adsorbed on the interface and self-assemble to form the thread-like pattern. The essential characteristics of this pattern formation are theoretically reproduced by a simple Monte Carlo simulation that takes into account the kinetics in the coalescence of charged micelles on a 2D interface. © 2012 American Institute of Physics. [<http://dx.doi.org/10.1063/1.4722079>]

I. INTRODUCTION

Spontaneous pattern formation on a mesoscopic scale has been attracting much attention from both scientific and industrial viewpoints. Mesoscopic structures in soft systems are often organized through a combination of short-range attraction and long-range electrostatic repulsion. The mechanism of pattern formation is usually interpreted in terms of a free-energy minimum. On the other hand, many studies have focused on unique structures generated as a kinetically trapped state, as represented by a fractal pattern.^{1,2} Nevertheless, most of the patterns on a mesoscopic scale may not represent either a pure thermodynamic manifestation or a pure kinetically trapped state. In other words, most mesoscopic structures are expected to be better interpreted as a product of both thermodynamics and kinetics. Thus, it would be of scientific importance to study pattern formation in a mesoscopic scale in terms of collaboration between these influences.³

Lipid molecules exhibit various kinds of mesoscopic structures, such as micelles (nm scale), lamellae (nm- μ m scale), and vesicles (μ m scale). A large number of experimental and theoretical studies mostly on electrically neutral lipids have been carried out, and these mesoscopic structures are now well interpreted in terms of statistical thermodynamics.⁴ Contrary to the mesoscopic structures with electrically neutral materials,⁵⁻⁸ we can expect that electrically charged lipid molecules will give novel structures. In such systems, cross talk between different levels of hierarchy, e.g., electrostatic interaction in the ionic atmosphere, is expected to provoke the formation of exotic mesoscopic structures. For example, lipid bilayer vesicles that contain negatively charged phospholipids exhibit micro-phase-separation that is stabilized by multivalent cations.^{9,10} Recently, in studies on mesoscopic lipid membrane structures, we have been studying the physicochemical characteristics of W/O droplets covered by phospholipid layers, which achieve small compartmentalization

as a simple model of a cell membrane. It has been shown that proteins and DNA molecules, which are both polyelectrolytes, exhibit unique properties inside W/O droplets that are similar in size to living cells, on the order of several tens of μ m.¹¹⁻¹⁹ Extensive studies with charged lipids have shown that novel and interesting phenomena emerge at an oil/water interface divided by a monolayer of charged phospholipids.

In the present study, we adopted W/O droplets with a negatively charged phospholipid. This system is regarded as a 2D oil/water interface with lipid membranes embedded in the 3D bulk oil phase with inverted lipid micelles that are sub- μ m-sized scale. We observed the spontaneous formation of a thread-like pattern on the oil/water interface under these experimental conditions, which was driven by the combined effect of thermodynamics and kinetics. Time-course analyses of fluorescence images and a numerical study that adopted a simple theoretical model were used to interpret the mechanisms of the formation of the thread-like pattern.

II. EXPERIMENTAL SECTION

A. Materials

Electrically neutral lipids, dipalmitoylphosphatidylcholine (DPPC; purity >99%) and dioleoylphosphatidylcholine (DOPC; purity >99%), were purchased from Wako Pure Chemical Industries (Osaka, Japan). A negatively charged lipid, dioleoylphosphatidylserine (DOPS; sodium salt; purity ~95%), and cholesterol (Chol; purity >99%) were purchased from Sigma-Aldrich Co. (St. Louis, MO). 1,2-Dioleoyl-*sn*-glycero-3-phosphoethanolamine-N-(lissamine rhodamine B sulfonyl) (Rho-PE) from Avanti Polar lipids (Alabaster, AL) was used as a fluorescent dye. All lipids were used without further purification and stored in powder form at -20 °C until use.

B. Preparation and observation of water-in-oil (W/O) droplets

The W/O droplets were prepared as described previously.¹⁴ First, neutral lipids and Chol were dissolved

^{a)} Author to whom correspondence should be addressed. Electronic mail: ichi@scphys.kyoto-u.ac.jp.

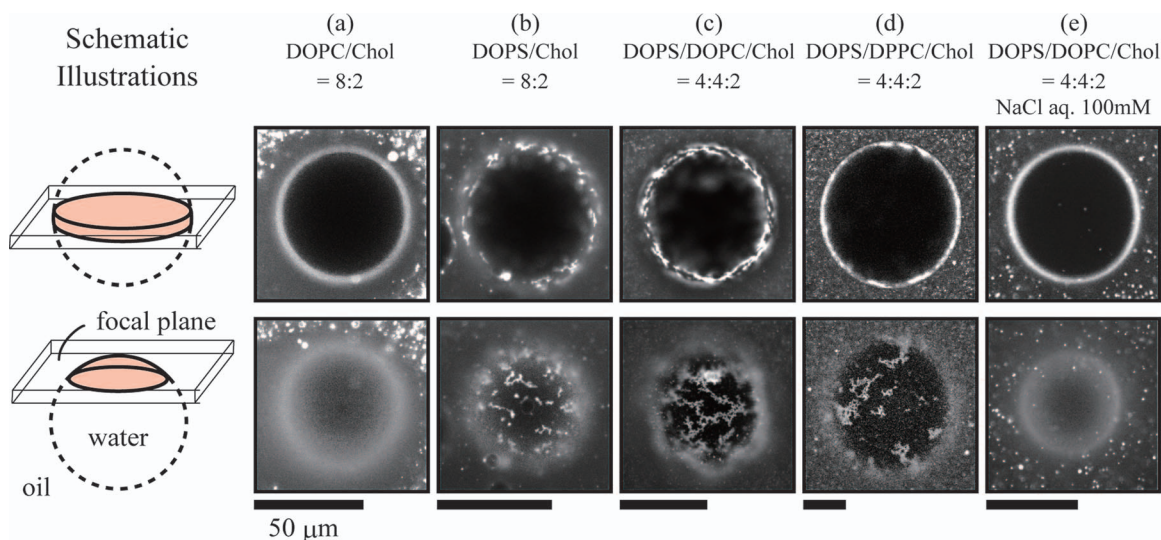


FIG. 1. Confocal microscopic images of W/O droplets at different focal planes with compositions of (a) DOPC/Chol = 8:2, (b) DOPS/Chol = 8:2, (c) DOPS/DOPC/Chol = 4:4:2, (d) DOPS/DPPC/Chol = 4:4:2, and (e) DOPS/DOPC/Chol = 4:4:2 that aqueous solution is NaCl aq. 100 mM. These pictures were captured at around 15–30 min after the samples were prepared. All scale bars correspond to 50 μm .

in chloroform, and the charged lipid DOPS was dissolved in chloroform/methanol (1:1) to be 10 mM, respectively. The molar ratio of Rho-PE was $\sim 0.75\%$ of the total lipid concentration. Next, the lipid solution with an appropriate composition was dried in a nitrogen stream and allowed to settle under vacuum overnight. In this process, the lipid mixture formed a dried lipid film. Third, mineral oil (Nacalai Tesque; Kyoto, Japan) was added to the lipid films to be 1 mM, and films were then sonicated at 50 $^{\circ}\text{C}$ for 90 min, which resulted in dispersed lipids in oil. Finally, to obtain W/O droplets, 5–10 vol% aqueous solution was added to the lipids in oil solution, and emulsification was performed by pipetting. The obtained droplets were observed using a confocal laser-scanning microscope (LSM510, Carl Zeiss; Jena, Germany) at room temperature.

III. RESULTS

A. Emergence of a thread-like pattern with a charged lipid

Figure 1 shows fluorescence images of W/O droplets coated with different types of lipids, where the upper and lower rows are cross-sectional and surface images of the droplets, respectively. These images were obtained within 30 min after preparation.

When the lipid composition was changed using electrically neutral lipids (DOPC, DPPC, Chol) and a negatively charged lipid (DOPS), a thread-like pattern was only observed in the presence of DOPS (Figs. 1(b)–1(d)). Interestingly, (b) DOPS/Chol = 8:2, (c) DOPS/DOPC/Chol = 4:4:2, and (d) DOPS/DPPC/Chol = 4:4:2 gave threads with similar shapes and time of emergence. The thread structure themselves were stable for more than several days, whereas the inverted-micelles in 3D bulk oil phase formed large clusters through aggregations. In addition, we also confirmed that the dye Rho-PE itself did not form such a pattern in a neutral lipid composition, as shown in Fig. 1(a).

It is known that the dye Rho-PE localizes on a liquid-disordered phase that is rich in unsaturated lipids (DOPS or DOPC).²⁰ Thus, it is expected that the thread-like pattern is mainly composed of DOPS, indicating that DOPS plays the main role in the formation of the thread-like pattern. In the following time-course analysis of pattern formation, we used the stable ternary system (c) DOPS/DOPC/Chol = 4:4:2 to examine the effect of electrostatic interaction in the simpler system since DOPS and DOPC had the same hydrophobic groups.

Figure 1(e) shows a result with a 100 mM NaCl solution. Although the oil and lipid composition were the same to those in Fig. 1(c), in which the thread-like pattern appeared, the oil/water interface clearly exhibited a homogeneous lipid layer in the presence of monovalent ions. This result indicates that thread-like pattern is generated through the electrostatic repulsion between negatively charged phospholipids DOPS, and the screening effect by monovalent cations inhibits the pattern formation.

B. Time-development of the interfacial pattern

Figure 2 shows an example of the time-development of the thread-like pattern observed in the cross-sectional images, which were captured at 1, 5, 11, and 15 min after sample preparation. The profiles on the right-hand side in Fig. 2(a) show the fluorescence intensity with a sampling size of $2\pi/360$ at each time vs. circumference distance λ obtained along the white arrow depicted in the first image. Backgrounds have been normalized. The temporal increase in the amplitude of intensity reflects the gradual localization of a Rho-PE-and-DOPS-rich phase.

On the other hand, void region between two adjacent peaks increased with time. This result means a growth of pattern spacing to a characteristic size, which was caused by diffusion of Rho-PE-and-DOPS-rich regions on the interface of a W/O droplet.

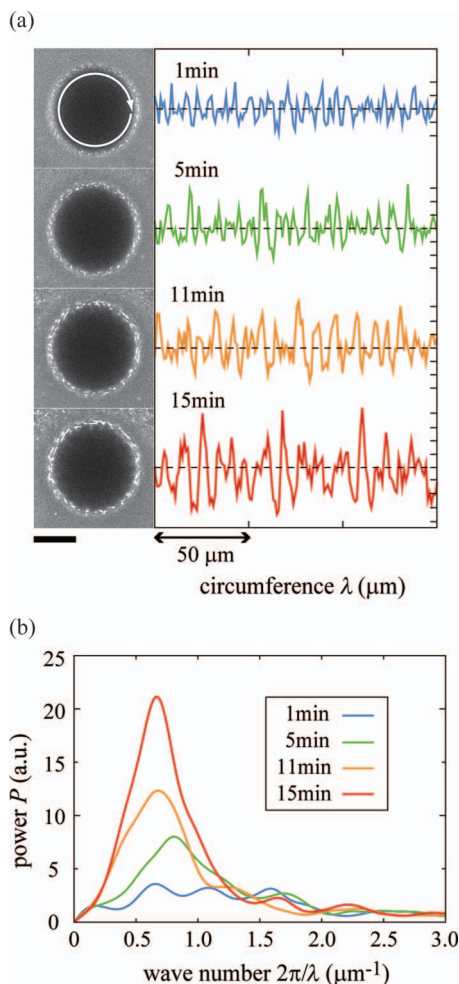


FIG. 2. Time-course of the pattern on the interface of a W/O droplet at DOPS/DOPC/Chol = 4:4:2, as revealed by fluorescence microscopy. (a) (Left) Cross-sectional images of the droplet with the pattern at each time. Scale bar is 50 μm. (Right) Profiles of fluorescence intensities along the circular circumference line as depicted by the white arrow. (b) Power spectra P of fluorescence intensity vs. wave number $2\pi/\lambda$.

Figure 2(b) shows the power spectra vs. wave number $k = 2\pi/\lambda$ μm⁻¹ at each time, calculated as

$$P(k) \equiv \left| \sum_{\lambda} I(\lambda) e^{-ik\lambda} \right|^2. \quad (1)$$

Each point was applied to a binomial smoothing over the range of $\Delta k \sim 1.3$ μm⁻¹ to capture the essential tendency from the discrete data obtained by fast-Fourier transform. The spectrum change indicates that the peak at around $k \approx 0.6$ μm⁻¹ grows with time, which corresponds to a spatial period of ≈ 10 μm. Thus, the width of the thread-like pattern has a characteristic length of $\lambda \approx 10$ μm. Figure 2(b) also shows the increase in the area of the peak at around $k \approx 0.6$ μm⁻¹, which reflects the growth of a thread-like pattern accompanied by the gradual adsorption of micelles in the oil phase onto the 2D interface of W/O droplets.

C. Kinetics on the adsorption of micelles in the oil phase onto the interface

Figure 3(a) shows the time-development of fluorescence images in the oil phase near the interface. The time-

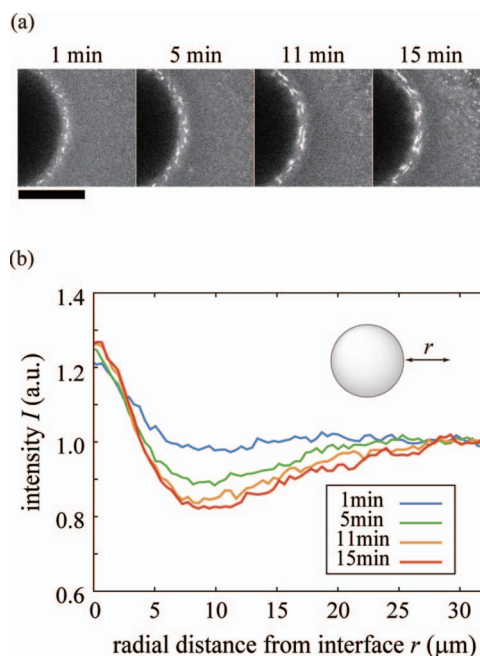


FIG. 3. Time-course of fluorescence intensity near the interface of the droplet, measured along the radial distance. (a) Fluorescence images near the interface. Scale bar is 50 μm. (b) Change in fluorescence intensity I over time, which was evaluated as the spatial average along the circle, vs. radial distance r from the interface of the W/O droplet.

development of the radial distribution function of fluorescence intensity is shown in Fig. 3(b), which corresponds to the density of the lipid molecules. As in Fig. 2, the radial intensity at the interface gradually increases with time. On the other hand, the intensity in the oil phase within 30 μm from the interface exhibits a marked decrease within 15 min after sample preparation.

This indicates that lipid micelles in the bulk region within 30 μm from the interface were gradually adsorbed onto the interface.

IV. DISCUSSION

A. Adsorption of micelles onto the interface through 3D diffusion in the bulk oil phase

The adsorption of micelles is considered to occur when they reach the interface by 3D diffusion in the bulk oil phase, where the characteristic length of diffusion is on the order of 30 μm in 15 min, as mentioned above. From the basic characteristics of diffusion caused by thermal fluctuation, we can write the diffusion coefficient of micelles in oil as $D \sim (\Delta x)^2/\Delta t$, where Δx and Δt are the characteristic diffusion length of a micelle and the observation time, respectively. Based on a consideration of the diffusion length $\Delta x \sim 10$ μm in a period of $\Delta t \sim 10^3$ s, the order of magnitude of the diffusion coefficient is expected to be $D \sim 10^{-9}$ cm² s⁻¹.

On the other hand, D of micelles in the oil can be approximately described by the Einstein relationship as $D = k_B T/6\pi\eta R$, where $6\pi\eta R$ is Stokes' friction coefficient. k_B , T , η , and R are the Boltzmann constant, absolute temperature, viscosity of the mineral oil, and the radius of a micelle, respectively. If we adopt the values $\eta \sim 2 \times 10^{-3}$ Pa s and

$D \sim 10^{-9} \text{ cm}^2 \text{ s}^{-1}$ to approximate the order of magnitude of the radius of a micelle R , we obtain an estimate of $R \sim 100 \text{ nm}$ at room temperature $T \sim 300 \text{ K}$. The radius estimated here is consistent with the widely known size of an inverted lipid micelle (or a small emulsion).^{21,22} This estimation reveals that the adsorption of micelles from the bulk oil phase onto the interface results from 3D diffusion, and their radii are $R \sim 100 \text{ nm}$. The supply of micelles from the 3D bulk to the 2D interface, as discussed here, adds a key kinetic effect to the system.

B. Characteristic thread-like pattern

Figure 2(b) clearly shows that the obtained thread-like pattern has a characteristic wave number of $2\pi/\lambda \approx 0.6 \mu\text{m}^{-1}$, i.e., it has a characteristic length of $\approx 10 \mu\text{m}$. The existence of such a characteristic length for the pattern means that the present pattern is definitely different from a fractal pattern. Typical fractal patterns can be obtained by the process of diffusion-limited aggregation (DLA), which forms a branched-string pattern without a characteristic length.²³ Recently, fractal aggregations of phosphatidylserine-vesicle-dispersions formed by a DLA process have been confirmed.²⁴ On the other hand, the thread-like assemblies of small colloids were observed in strong external fields, while linear assembly is driven by asymmetric non-equilibrium fields.^{25,26} Although the above mentioned systems exhibiting inherent asymmetric elements or anisotropic external field generate ordered or thread-like patterns of small elements through kinetic processes, the mechanisms considered in these previous works cannot reproduce the essential features observed in the present experiments, i.e., formation of the thread-like pattern with a certain characteristic length in the absence of any specific internal and external field.

Based on the experimental results shown in Figs. 1–3, the thread-like pattern is formed as a result of the contributions from both the adsorption of charged lipid micelles onto the interface from the bulk (see Fig. 3), and their 2D diffusion on the interface (see Fig. 2). From this point of view, we need to understand what occurs in the interaction between charged micelles to reveal the mechanism of thread-like pattern formation. This interaction between charged micelles provides a thermodynamic effect to the system.

C. Numerical simulation

To shed light on the mechanism of the thread-like pattern formation, we performed 2D biased Metropolis Monte Carlo simulations for a simple numerical model. Here, we modeled the assembly process of small particles on 2D plane in order to extract the essence of the mechanism concerning the thread-like pattern formation of micelles on an oil/water interface, since diameters of water droplets are large enough compared to those of micelles. As shown in Fig. 4(a), a thread-like assembly was obtained under the supply of particles and competing interactions between a short-range attractive interaction and a long-range repulsive interaction. The short-range attraction and the long-range repulsion are strong hydrophobic attraction between the alkyl chains of inverted micelles,

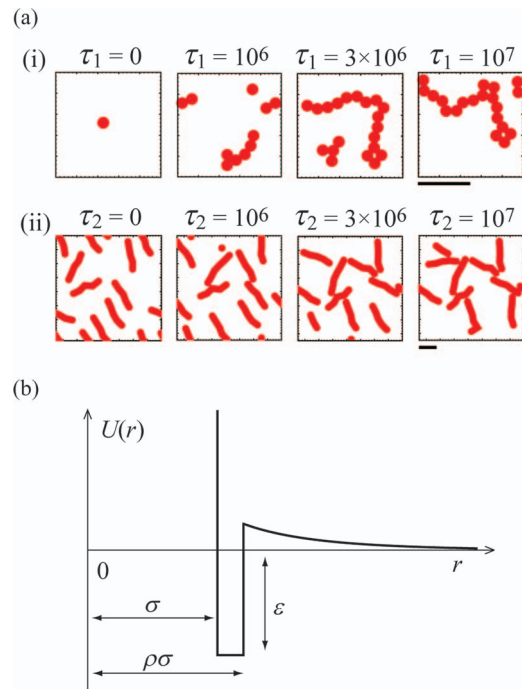


FIG. 4. (a) The results of the numerical simulation on the formation of a thread-like pattern obtained by the Monte Carlo method; (i) a thread composed of particles in early process and (ii) a branched thread-like pattern composed of coarse-grained threads in late process, after each Monte Carlo steps τ_1 and τ_2 , respectively. In early process (i), we set a time-constant increase in micelles of 1 per 10^5 steps. Scale bars correspond to 5σ in both (i) and (ii). (b) Schematic illustration of the potential profile in Eq. (2).

which is on the order of nm, and screened electrostatic repulsive interaction between negatively charged micelles, which is modeled by the Yukawa potential, respectively. In this model, the detailed potential energy between two micelles is given by

$$U(r) = U_{att}(r) + U_{rep}(r) = \begin{cases} \infty, & \text{for } r < \sigma \\ -\varepsilon, & \text{for } \sigma \leq r < \rho\sigma \\ C \frac{e^{-r/l_D}}{r/\sigma}, & \text{for } \rho\sigma \leq r, \end{cases} \quad (2)$$

where r , l_D , and σ are the center-to-center distance between two micelles, the Debye length in the bulk oil, and the diameter of a micelle, respectively. ε and C are parameters that represent the depth of the attractive well potential and the height of the screened repulsive potential. ρ determines the range of short-range attraction. The total potential is described as shown in Fig. 4(b).

To describe the coalescence of inverted micelles on the order of 100 nm ($=\sigma$), the values $\rho = 1.03$, $\varepsilon = 1000 k_B T$, $l_D = 100 \text{ nm}$, and $C = 10 k_B T$ are adopted for the strong short-range hydrophobic attraction and the long-range repulsion. This simple well potential exhibits the combination of short-range attraction and long-range repulsion, which represents qualitative features of common models such as Derjaguin-Landau-Verwey-Overbeek interaction.^{27,28}

To clarify the thread-like clustering of charged particles and the slow assembling of the clusters, a two-stage process of pattern formation in different time scales is proposed; (i) early process: charged particles on a 2D surface, which mimic

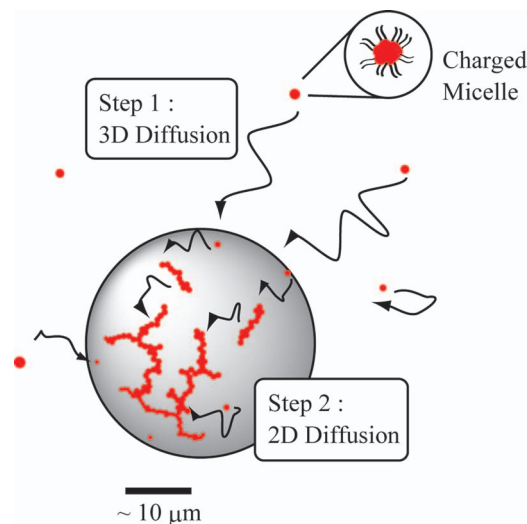


FIG. 5. Schematic illustration of the mechanism of thread-like pattern formation. In Step 1, micelles in the 3D oil phase undergo random walk and gradually fall on the interface of a droplet. In Step 2, they diffuse on the 2D surface of the droplet and collide/stick with each other to form a thread-like pattern.

charged micelles at the interface of a W/O droplet, coalesce into threads under Brownian motion, and (ii) late process: coarse-grained rigid threads coalesce into a larger thread accompanied by the formation of branches. In early process (i), micelles in an aggregate were allowed rearrangements to represent an annealing process. To represent the gradual adsorption of micelles, we linearly increase the number of particles from 2 as an initial condition, which occupies 1.6% of the area, to 20 as a final condition, which results in a 10-fold greater particle density than the initial value. Microscopic structures generated in this process are, thus, expected to be formed through the competition of short-range attraction and long-range repulsion under constant supply of particles from 3D bulk. In late process (ii), coarse-grained threads stick together to form a larger scale structure. In this calculation, the volume fraction of threads was constant corresponding to the experimental observation of the long-time behavior. With a small displacement M of the particles and the threads, they can mimic Brownian particles in a fluid with random trial motion.²⁹ By taking into account the calculation stabilities, we adopted $M = 0.5$ and 0.01 as the maximum absolute values of a fluctuation in 1 Monte Carlo step in processes (i) and (ii), respectively.

According to the above mentioned conditions, the results compatible with the experimental thread-like pattern are obtained under the contribution of thermodynamics represented by the competition between interactions of different ranges, and kinetics represented by the supply of particles and sticky potential. The scenario of the pattern formation reported in the present study is expected to shed light on the generation mechanisms of various assemblies of nanoparticles or biological macromolecules on 2D interface.^{30,31}

V. SUMMARY

The present results showed that the thread-like pattern is spontaneously generated at the interface of W/O droplets in

the presence of negatively charged lipid DOPS. Charged lipid micelles in the bulk oil phase gradually adsorb onto the interface, and the thread-like pattern then grows in size over time until it reaches a characteristic size through the coalescence of micelles in the early process. As the late process, the clusters form a branched thread-like shape at the 2D interface with long-range repulsion such as electrostatic interaction. The overall mechanism of pattern formation is schematically represented in Fig. 5. Since conventional systems that exhibit pattern formation (e.g., colloidal gels) have been studied from the viewpoint of a constant number of particles, the mechanism that produces a thread-like pattern accompanied by the kinetic process of a time-dependent increase in mesoscopic particles may inspire the future extension of this perspective to studies on spontaneous pattern formation in soft materials; for example, pattern generation on supported membranes^{32,33} or Pickering emulsions.^{34–36}

ACKNOWLEDGMENTS

This work was supported by grants from Kyoto University Venture Business Laboratory (grants-in-aid program for young researchers), the Ministry of Education, Culture, Sports, Science and Technology (Research Activity Start-up, No. 23840031; Scientific Research on Innovative Areas, No. 23106712), and the JSPS Core-to-Core Program “International research network for non-equilibrium dynamics of soft matter.”

¹L. W. Anacker and R. Kopelman, *J. Chem. Phys.* **81**, 6402 (1984).

²R. Kopelman, *J. Stat. Phys.* **42**, 185 (1986).

³E. Zaccarelli, *J. Phys.: Condens. Matter* **19**, 323101 (2007).

⁴J. N. Israelachvili, *Intermolecular and Surface Forces*, 3rd ed. (Academic, London, 2011).

⁵S. L. Veatch and S. L. Keller, *Phys. Rev. Lett.* **89**, 268101 (2002).

⁶R. Lipowsky and R. Dimova, *J. Phys.: Condens. Matter* **15**, 31 (2003).

⁷M. Yanagisawa, M. Imai, and T. Taniguchi, *Phys. Rev. Lett.* **100**, 148102 (2008).

⁸M. Yanagisawa, M. Imai, and T. Taniguchi, *Phys. Rev. E* **82**, 051928 (2010).

⁹C. C. Vequi-Suplicy, K. A. Riske, R. L. Knorr, and R. Dimova, *Biochim. Biophys. Acta* **1798**, 1338 (2010).

¹⁰N. Shimokawa, M. Hishida, H. Seto, and K. Yoshikawa, *Chem. Phys. Lett.* **496**, 59 (2010).

¹¹A. Kato, M. Yanagisawa, Y. T. Sato, K. Fujiwara, and K. Yoshikawa, *Sci. Rep.* **2**, 283 (2012).

¹²M. Hase and K. Yoshikawa, *J. Chem. Phys.* **124**, 104903 (2006).

¹³M. Hase, A. Yamada, T. Hamada, D. Baigl, and K. Yoshikawa, *Langmuir* **23**, 348 (2007).

¹⁴A. Kato, E. Shindo, T. Sakaue, A. Tsuji, and K. Yoshikawa, *Biophys. J.* **97**, 1678 (2009).

¹⁵T. Hamada, M. Morita, Y. Kishimoto, Y. Komatsu, M. Vestergaard, and M. Takagi, *J. Phys. Chem. Lett.* **1**, 170 (2010).

¹⁶M. K. Krotova, V. V. Vasilevskaya, N. Makita, K. Yoshikawa, and A. R. Khokhlov, *Phys. Rev. Lett.* **105**, 128302 (2010).

¹⁷A. Kato, A. Tsuji, M. Yanagisawa, D. Saeki, K. Juni, Ya. Morimoto, and K. Yoshikawa, *J. Phys. Chem. Lett.* **1**, 3391 (2010).

¹⁸M. Negishi, M. Ichikawa, M. Nakajima, M. Kojima, T. Fukuda, and K. Yoshikawa, *Phys. Rev. E* **83**, 061921 (2011).

¹⁹M. Yanagisawa, M. Iwamoto, A. Kato, K. Yoshikawa, and S. Oiki, *J. Am. Chem. Soc.* **133**, 11774 (2011).

²⁰A. V. Samsonov, I. Mihalyov, and F. S. Cohen, *Biophys. J.* **81**, 1486 (2001).

²¹N. A. Mazer, G. B. Benedek, and M. C. Carey, *Biochemistry* **19**, 601 (1980).

²²P. Walde, A. M. Giuliani, C. A. Boicelli, and P. L. Luisi, *Chem. Phys. Lipids* **53**, 265 (1990).

²³T. A. Witten and L. M. Sander, *Phys. Rev. Lett.* **47**, 1400 (1981).

- ²⁴S. Roldan-Vargas, A. Martin-Molina, M. Quesada-Perez, R. Barnadas-Rodriguez, J. Estelrich, and J. Callejas-Fernandez, *Phys. Rev. E* **75**, 021912 (2007).
- ²⁵M. Ichikawa, Y. Matsuzawa, Y. Koyama, and K. Yoshikawa, *Langmuir* **19**, 5444 (2003).
- ²⁶W. D. Ristenpart, I. A. Aksay, and D. A. Saville, *Phys. Rev. Lett.* **90**, 128303 (2003).
- ²⁷B. V. Derjaguin and L. Landau, *Acta. Physicochim. USSR* **14**, 633 (1941).
- ²⁸E. J. W. Verwey and J. T. G. Overbeek, *Theory of the Stability of Lyophobic Colloids* (Elsevier, Amsterdam, 1948).
- ²⁹K. Kikuchi, M. Yoshida, T. Maekawa, and H. Watanabe, *Chem. Phys. Lett.* **185**, 335 (1991).
- ³⁰A. Saric and A. Cacciuto, *Phys. Rev. Lett.* **108**, 118101 (2012).
- ³¹M. Morita, T. Hamada, Y. Tendo, T. Hata, M. C. Vestergaard, and M. Takagi, *Soft Matter* **8**, 2816 (2012).
- ³²E. Sackmann and M. Tanaka, *Trends Biotechnol.* **18**, 58 (2000).
- ³³C. Dietrich, Z. N. Volovyk, M. Levi, N. L. Thompson, and K. Jacobson, *Proc. Natl. Acad. Sci. U.S.A.* **98**, 10642 (2001).
- ³⁴S. U. Pickering, *J. Chem. Soc.* **91**, 2001 (1907).
- ³⁵M. F. Hsu, M. G. Nikolaides, A. D. Dinsmore, A. R. Bausch, V. D. Gordon, X. Chen, J. W. Hutchinson, and D. A. Weitz, *Langmuir* **21**, 2963 (2005).
- ³⁶M. Grzelczak, J. Vermant, E. M. Furst, and L. M. Liz-Marzan, *ACS Nano* **4**, 3591 (2010).